Pergamon

Int. J. Heat Mass Transfer. Vol. 40, No. 7, pp. 1567–1576, 1997

0017–9310/97 $17.00+0.00

PII: S0017–9310(96)00217–7

Effects of a porous medium on local heat transfer and fluid flow in a forced convection field

KOICHI ICHIMIYA and TAKESHI MATSUDA

Department of Mechanical System Engineering, Yamanashi University, Takeda-4, Kofu, Yamanashi 400, Japan

and

YASUYUKI KAWAI

Takagi Industry Co Ltd, Nishikashiwabarashinden-201, Fuji, Shizuoka 417, Japan

(*Received* 19 *January* 1996 *and in final form* 12 *June* 1996)

Abstract—A numerical estimation was made for the laminar flow and heat transfer through a porous medium placed in a flow passage with a miter bend. Heat transfer between solid material and fluid was considered in the numerical analysis. The calculations were performed for the Darcy number $Da = 1$–2.5×10^{-6}, the ratio of thermal conductivity of solid material to fluid $RRM = 1$–1000, the parameter for heat transfer between solid material and fluid $H_g = 10$–1000 and the Reynolds number $Re = 300$. The results of local heat transfer and dimensionless stream function were compared for the cases with and without a porous medium. The behavior of the flow, the solid and gas temperatures, the Nusselt number with these parameters and the thermal performance were illustrated. It was found that a porous medium with high RRM and H_g should be selected with an optimum Darcy number to enhance the local heat transfer without a significant flow resistance. Copyright © 1996 Elsevier Science Ltd.

INTRODUCTION

A porous medium has been applied to the control of heat transfer in various ways. We have experimentally and numerically investigated heat transfer characteristics at room temperature in the case where a porous medium is placed in a channel as a turbulence promoter, which causes only a low pressure drop [1, 2]. Thus, the effectiveness of using a porous medium to improve the heat transfer has been confirmed. In order to make the best of the experience gained through these studies and to advance the application of porous media to heat storage type heat exchangers, regenerators and filters in Stirling engines, it is essential to analyze how the local flow and heat transfer can be controlled by placing a porous medium in a forced convection dominated field. Kaviany studied heat transfer characteristics when a porous medium was placed in a channel of parallel plates, both of which were heated to a constant temperature [3], and when such a medium was placed on a semi-infinite plate with uniform temperature [4]. Also, Poulikakos *et al.* studied the distributions of velocity, Nusselt number and pressure gradient along the flow directions in a channel partially filled with a porous medium, which was placed to cover the heated wall [5] and which was installed in the center of the flow passage locally [6]. Furthermore, Hunt *et al.* experimentally analyzed the heat propagation through a fibrous medium and evaluated average heat transfer along the flow direction [7]. In these studies straight ducts were used and heat diffusion inside a porous medium was evaluated using the effective thermal conductivity of the fluid-saturated porous medium.

In the present study, we use a flow passage with a miter bend; a porous medium is placed downstream of the bend and the effects of the medium on the local flow and heat transfer are numerically analyzed. In the study, heat transfer between the solid medium and fluid is taken into consideration. A bent duct was selected as a flow passage because a duct containing bends elucidates the effect of a porous medium more clearly than does a straight duct.

DESCRIPTION OF THE PROBLEM

Figure 1 shows a schematic diagram of the system used in the present study. The flow passage system consists of parallel plates whose upper edge is designated as the origin of x- (horizontal) and y- (vertical) axes. The height of the inlet and exit is set to y_0. Fluid enters the inlet of the duct with a laminar fully developed velocity distribution (parabola distribution). The fluid enters the bend section after passing

NOMENCLATURE

A_s	surface area of a solid particle
Da	Darcy number $= K/h^2$
h	width of porous medium $= 2y_0$
h_A	heat transfer coefficient between solid material and fluid
H	dimensionless width $= h/y_0$
H_g	dimensionless parameter $= h_A n_s A_s y_0^2/\lambda_g$
H_s	dimensionless parameter $= H_g(\lambda_g/\lambda_s)$
K	permeability
n_s	number of solid particles in unit volume
Nu	Nusselt number $= \alpha \cdot 2y_0/\lambda_g$
Pr	Prandtl number
q	heat flux
Re	Reynolds number $= u_m \cdot 2y_0/\nu$
RRM	thermal conductivity ratio $= \lambda_s/\lambda_g$
T	temperature
T_0	fluid temperature at entrance
T_w	heated wall temperature
u	velocity along x-direction
u_m	mean velocity across the section
U	dimensionless velocity along x-direction
v	velocity along y-direction
V	dimensionless velocity along y-direction
X	dimensionless coordinate $= x/y_0$
y_0	width of flow passage at entrance
Y	dimensionless coordinate $= y/y_0$.

Greek symbols

α	heat transfer coefficient between heated wall and fluid
ε	porosity
Θ	dimensionless temperature (refer to equation (1))
ψ	stream function
Ψ	dimensionless stream function (refer to equation (1))
ω	vorticity
Ω	dimensionless vorticity (refer to equation (1))
λ	thermal conductivity
μ	viscosity
$\tilde{\mu}$	effective viscosity of porous medium
ν	kinetic viscosity.

Subscripts

g	fluid
s	solid.

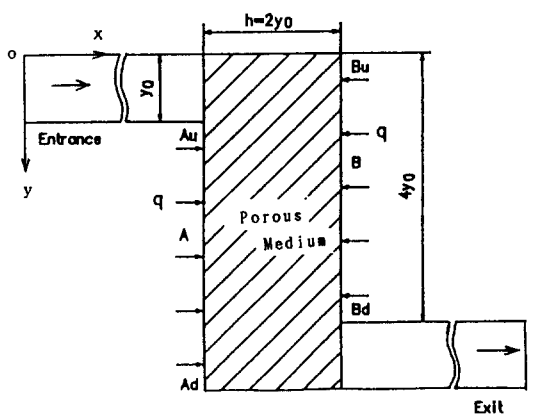

Fig. 1. Coordinate system.

the $10y_0$ straight section. A porous medium is placed to cover the duct height h ($=2y_0$) and its length $5y_0$ in the y-direction. Sidewalls are heated on both upstream side walls (Au-Ad) and downstream side wall (Bu-Bd) under the uniform heat flux, q. The fluid flow further develops after passing through the bend section and straight section which extends over the downstream section $50y_0$. Furthermore, nonheated walls are thermally insulated. Considering the medium as a mass of spherical particles, we set the porosity, permeability, surface area of a particle, number of particles per unit volume and heat transfer coefficient between particles and fluid as ε, K, A_s, n_s and h_A, respectively. The momentum equations of the flow in the porous medium are constructed on the basis of the non-Darcy model in which the Brinkman term (viscous term) and Forchheimer term (inertia term) are included [8]. With respect to heat transfer field, thermal radiation is ignored, since heat conduction and convection dominate over it. Moreover, heat transfer between the porous medium and fluid is also considered. The thermal properties of the fluid and porous medium are assumed to be constant.

NUMERICAL ANALYSIS

The governing equations (flow and energy equations) can be written in the dimensionless form (equations (2)–(5)) by using the following parameters (equation (1)) including a stream function ψ and a vorticity ω. Here, subscripts g and s represent fluid and solid, respectively:

$$u = \frac{\partial \psi}{\partial y}, v = -\frac{\partial \psi}{\partial x}, \omega = \frac{\partial v}{\partial x} - \frac{\partial u}{\partial y},$$

$$\Psi = \frac{\psi}{y_0 u_m}, \Omega = \frac{\omega y_0}{u_m}, \Theta_{g,s} = \frac{\lambda_g (T_{g,s} - T_0)}{q y_0}. \quad (1)$$

Flow equations

$$\frac{\partial^2 \Psi}{\partial X^2} + \frac{\partial^2 \Psi}{\partial Y^2} = -\Omega \quad (2)$$

$$\frac{\partial \Psi}{\partial Y}\frac{\partial \Omega}{\partial X} - \frac{\partial \Psi}{\partial X}\frac{\partial \Omega}{\partial Y} = \frac{2\varepsilon}{Re}\frac{\tilde{\mu}}{\mu}\left(\frac{\partial^2 \Omega}{\partial X^2} + \frac{\partial^2 \Omega}{\partial Y^2}\right) - \frac{2\varepsilon^2 \Omega}{Re\, H^2 Da} - \frac{\varepsilon^2 C}{H\sqrt{Da}}\left\{\frac{\partial}{\partial X}\left(\sqrt{\left(\frac{\partial \Psi}{\partial X}\right)^2 + \left(\frac{\partial \Psi}{\partial Y}\right)^2} \times \left(-\frac{\partial \Psi}{\partial X}\right)\right) - \frac{\partial}{\partial Y}\left(\sqrt{\left(\frac{\partial \Psi}{\partial X}\right)^2 + \left(\frac{\partial \Psi}{\partial Y}\right)^2}\left(\frac{\partial \Psi}{\partial Y}\right)\right)\right\}. \quad (3)$$

Energy equation

For the fluid:

$$\frac{\partial \Psi}{\partial Y}\frac{\partial \Theta_g}{\partial X} - \frac{\partial \Psi}{\partial X}\frac{\partial \Theta_g}{\partial Y} = \frac{2}{Re\, Pr}\left(\frac{\partial^2 \Theta_g}{\partial X^2} + \frac{\partial^2 \Theta_g}{\partial Y^2}\right) - \frac{2H_g}{Re\, Pr}(\Theta_g - \Theta_s). \quad (4)$$

For the solid:

$$\frac{\partial^2 \Theta_s}{\partial X^2} + \frac{\partial^2 \Theta_s}{\partial Y^2} = H_s(\Theta_s - \Theta_g). \quad (5)$$

The value obtained by Ergun [9] is used for the coefficient C on the righthand side of equation (3),

$$C = (1.75/\sqrt{175})\varepsilon^{-1.5}.$$

Dimensionless parameters, Da, H_g and H_s are defined as follows:

$$Da = K/h^2, \quad H_g = h_A n_s A_S y_0^2/\lambda_g, \quad H_s = H_g(\lambda_g/\lambda_s)$$

where Da is the Darcy number and H_g is the dimensionless parameter of the medium, which represents the heat transfer between particles and fluid saturated in the porous medium. Depending on whether the porous medium is made of particles or nonparticles, different values h_A are used to represent heat transfer coefficient in a porous medium. It is of the order of 10^{-2} to 10^{-3} in terms of Nusselt number [10–12]. Considering the above fact, we assume H_g in the range of 10–1000 in this analysis. H_s corresponds to the Biot modulus on the solid particles. The thermal conductivity ratio of the solid to fluid λ_s/λ_g ($= RRM$) is between 10 and 1000 since a gas ($Pr = 0.7$) is used as a working fluid. However, for reference, calculations have been performed for $RRM = 1$.

Dimensionless boundary conditions are as follows:

- at entrance, $U = -6(Y^2 - Y)$, $V = 0$, $\Theta_g = 0$;
- at upper and bottom walls, $U = 0$, $V = 0$, $\partial\Theta_g/\partial Y = \partial\Theta_s/\partial Y = 0$;
- at side walls, Au-Ad $U = 0$, $V = 0$, $\partial\Theta_g/\partial X = RRM\partial\Theta_s/\partial X = -1$, Bu-Bd $U = 0$, $V = 0$, $\partial\Theta_g/\partial X = RRM\partial\Theta_s/\partial X = 1$;
- at exit, $\partial U/\partial X = 0$, $V = 0$, $\partial\Theta_g/\partial X = 0$;
- at interface, $\partial U/\partial X|_s = \partial U/\partial X$, $(\tilde{\mu}/\mu)\partial V/\partial X|_s = \partial V/\partial X$;

where $\tilde{\mu}/\mu$ is the ratio of effective viscosity of the saturated porous medium to fluid viscosity in the duct. Introducing the value used by Neal *et al.* [13], we used the value of $\tilde{\mu}/\mu = 1.2$ in the present study. With respect to the interface, the condition in the Neal–Nader case [13], wherein the flow and the interface are parallel, was applied for the flow along the y-direction.

Regarding numerical calculations, the governing equations are integrated and represented as a conservative system. The upwind scheme is employed for discretizing convection terms [14]. The wall vorticity is extrapolated using values of stream function on the three consecutive grid nodes near and on the wall. The algebraic equations are solved iteratively. The temperature gradient on the heated wall is also obtained by using the values at three grids near and on the wall. For the convergent condition, we used the criterion that the maximum absolute value differences between two successive values of the functions Ψ, Ω, and Θ at each grid point satisfy the following conditions:

$$\text{Max}\,|\phi^{(n)} - \phi^{(n-1)}| \leqslant 6 \times 10^{-4}$$

where ϕ represents Ψ, Ω or Θ.

Numerical calculations were performed at fixed values $Re = 300$ and $Pr = 0.7$, whereas the other parameters were varied, namely, the heat transfer parameter between solid particle and fluid, H_g (= 10–1000), the ratio of thermal conductivity, RRM (= 1–1000), and the Darcy number, Da (= 1 to 2.5×10^{-6}). The results obtained were examined in terms of the dimensionless stream function, Ψ, the dimensionless temperature, Θ and the Nusselt number, Nu,

$$Nu = 2qy_0/\{\lambda_g(T_w - T_0)\} = 2/\Theta_w.$$

RESULTS OF NUMERICAL CALCULATIONS

Figure 2 shows the results of dimensionless stream function Ψ for cases with and without the porous medium. When a porous medium is not present in the duct (Fig. 2(a)), the fluid with a fully developed laminar profile passes through the entrance and impinges to the surface (Bu-Bd). The direction of flow is altered by 90°. During this process, small vortices and large recirculating flow are produced on the right upper wall and on the (Au-Ad) side, respectively. The center of the recirculating flow is located on the down-

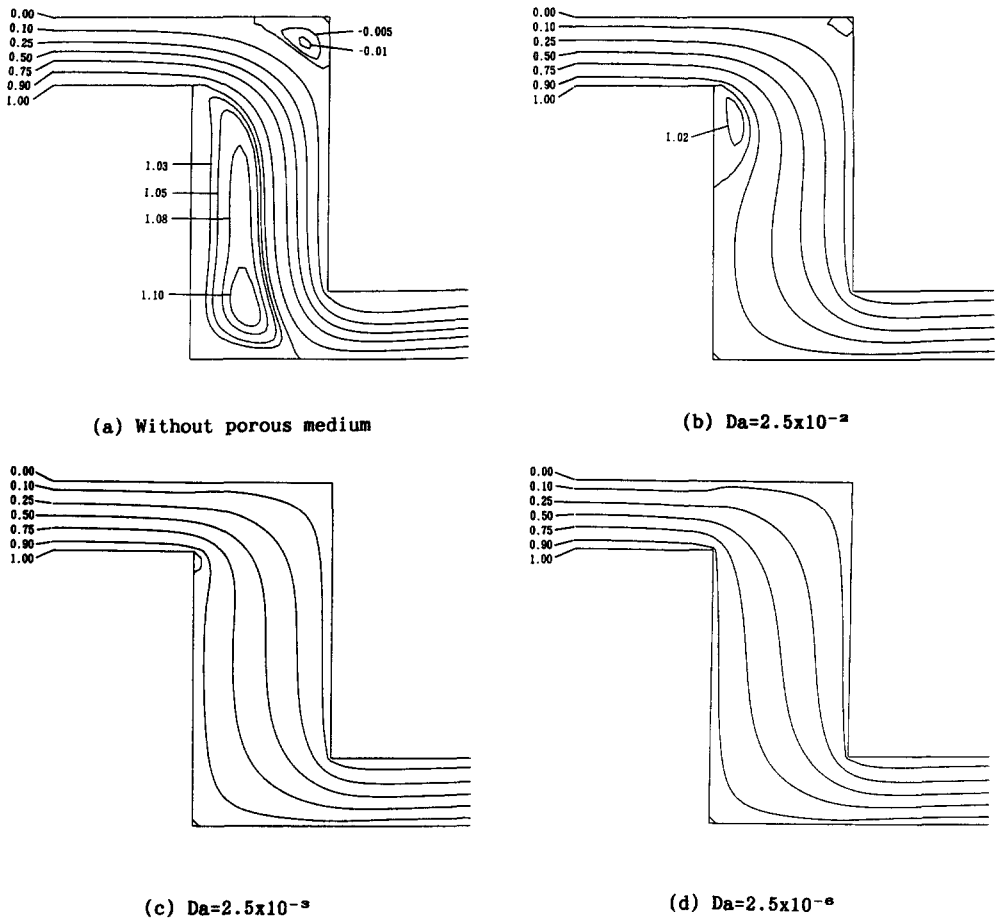

Fig. 2. Dimensionless stream function Ψ ($Re = 300$): (a) without porous medium; (b) $Da = 2.5 \times 10^{-2}$; (c) $Da = 2.5 \times 10^{-3}$; (d) $Da = 2.5 \times 10^{-6}$.

stream side; the flow on the (Bu-Bd) side is accelerated, changes its direction downstream, and enters into the straight section. At the exit, a small recirculating flow of the width y_0 develops in the upper section of the duct. Figure 2(b), (c) and (d) show dimensionless stream function in the duct obtained in the presence of a porous medium, changing Darcy number Da. At $Da = 2.5 \times 10^{-2}$, the size of recirculating flow decreases to one third of that without a porous medium, and the center of recirculating flow moves to an upstream position (edge of the bend). At $Da = 2.5 \times 10^{-3}$, a small vortex is observed on the (Au-Ad) side at the edge of the bend; however, at $Da = 2.5 \times 10^{-6}$, recirculating flow disappears and the flow becomes uniform well.

Figures 3 and 4 show the fluid and solid temperature distributions in the duct, respectively, obtained at $H_g = 100$ and $RRM = 100$ for different values of Da. Figure 3(a) shows the isotherms of fluid in the absence of a porous medium. The figure shows that, due to the effect of the recirculating flow on the (Au-Ad) side, the temperature over half of the width of the duct increases above $\Theta_g = 0.1$, and the isothermal lines initiating at the upper corner of the bend $\Theta_g = 0.01$–0.05 move toward the (Bu-Bd) side. When a porous medium is present in the duct under this condition, the temperature, as indicated by isothermal lines $\Theta_g = 0.01$–0.06, rises linearly downward (Fig. 3(b), (c) and (d)). The isotherms upstream of the bend do not change so much with the decrease in the Da number; however, the area with the temperature higher than $\Theta_g = 0.08$ increases. On the other hand, the temperature gradient in the porous medium (Fig. 4(a), (b) and (c)), near the heat transfer surface, is not as high as that in the fluid because of high thermal conductivity $RRM = 100$. The effect of the change in the Da number emerges downstream of the bend. With the decrease in the Da number, the region of high temperature expands in the vertical direction of the duct. Figure 5(a) and (b) show the local Nusselt number on the heated surface. The dash-chained line shows the case without a porous medium. On the (Au-Ad) side (Fig. 5(a)), heat transfer on the upstream side is remarkably promoted by the insertion of a porous medium, due to the reduction of the size of recirculating flow and its subsequent disappearance; the smaller the value of the Da number, the greater is the rate of improvement. On the downstream side, however, although the tendency is weak, the larger the Da number, the greater is the value of the Nu

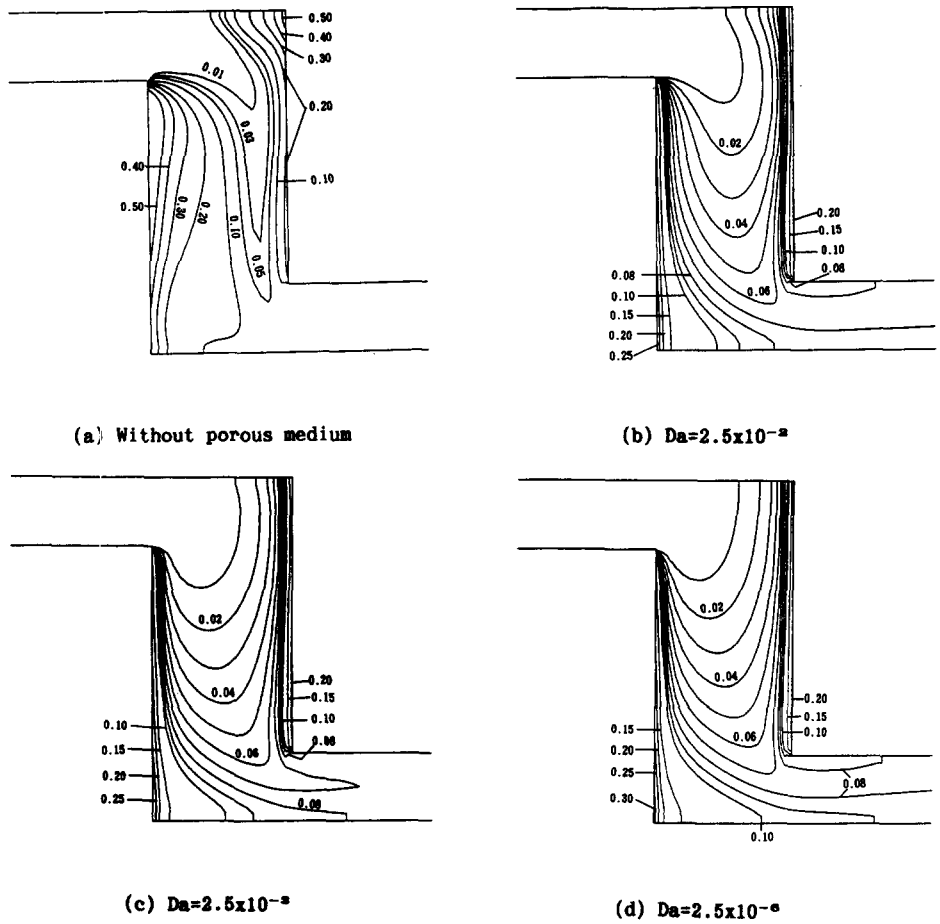

Fig. 3. Dimensionless fluid temperature Θ_g ($H_g = 100$, $RRM = 100$): (a) without porous medium; (b) $Da = 2.5 \times 10^{-2}$; (c) $Da = 2.5 \times 10^{-3}$; (d) $Da = 2.5 \times 10^{-6}$.

number. On the other hand, on the (Bu-Bd) side (Fig. 5(b)), heat transfer is enhanced upstream, up to the point close to $Y = 1.0$, but its enhancement diminishes thereafter. Figure 6 shows the average Nusselt number in the case of dual-side heating. The dashed line on the right-hand side of the figure shows the results for the (Bu-Bd) side when porous medium is not present. The fine dotted line shows the result for the (Au-Ad) side. The effectiveness of the insertion of a porous medium into the full height of the flow passage on the promotion of the heat transfer is approximately 2.5-fold on the (Au-Ad) side (symbol ○) and approximately 1.25-fold on the (Bu-Bd) side (symbol ▲), as compared to the case without a porous medium.

Figures 7 and 8 show the effect of the ratio of thermal conductivity RRM ($=\lambda_s/\lambda_g$) on the temperature distribution of the fluid and medium at $Da = 2.5 \times 10^{-3}$ and $H_g = 10$. When the value of RRM is large (Fig. 7(a)), the temperature rise near the center of the flow passage is mild due to heat

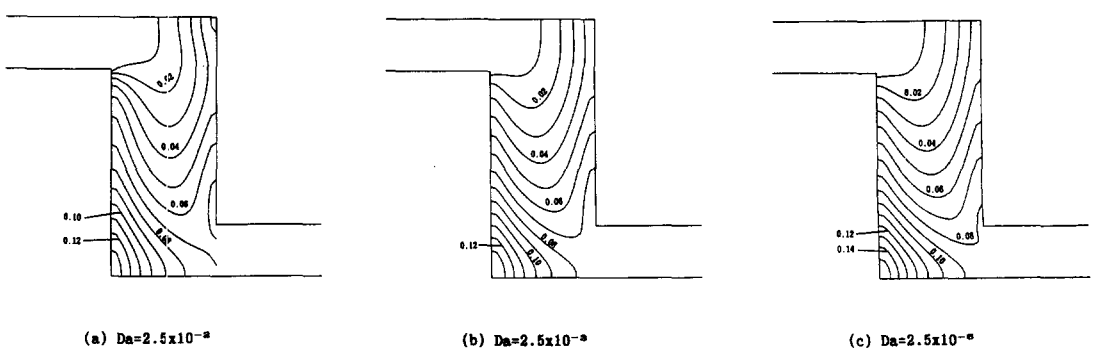

Fig. 4. Dimensionless solid temperature Θ_s ($H_g = 100$, $RRM = 100$): (a) $Da = 2.5 \times 10^{-2}$; (b) $Da = 2.5 \times 10^{-3}$; (c) $Da = 2.5 \times 10^{-6}$.

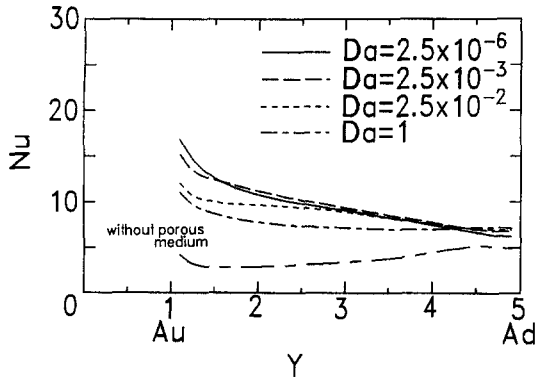

(a) (Au-Ad) side

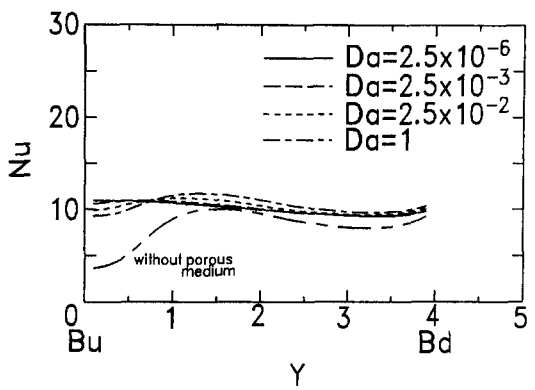

(b) (Bu-Bd) side

Fig. 5. Local Nusselt number ($H_g = 100$, $RRM = 100$): (a) (Au-Ad) side; (b) (Bu-Bd) side.

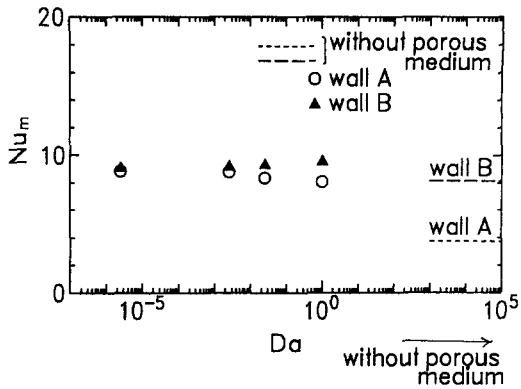

Fig. 6. Mean Nusselt number ($H_g = 100$, $RRM = 100$).

diffusion by the porous medium. The isotherm of $\Theta_g = 0.04$ extends downstream of the miter bend. This indicates that the thermal boundary layer, whose temperature gradient near the heated walls is large, is relatively thin. Conversely, when the value of RRM is small (Fig. 7(b)), tendency opposite to this is observed. The isotherm $\Theta_g = 0.04$ does not extend downstream and the temperature near the (Bu-Bd) side rises. With respect to the temperature of the porous medium (Fig. 8(a) and (b)), due to the direct effect of heat diffusion, the temperature of the entire flow passage increases for the case of small RRM. This means that heat storage is also promoted by a porous medium. The temperature distribution within the cross section is averaged out. Accordingly, the larger the value of RRM, the higher is the value of the local Nusselt number on the heated walls for both the (Au-Ad) side and (Bu-Bd) side (Fig. 9(a) and (b)). However, there is a section on the (Bu-Bd) side where the local heat transfer deteriorates as compared to the case without a porous medium. This happens when the heat transfer parameter between the porous medium and fluid, H_g, is too small.

Figures 10 and 11 show the effect of the heat transfer parameter between the porous medium and fluid, H_g, on temperature distributions of the fluid and porous medium, respectively, at $Da = 2.5 \times 10^{-3}$ and $RRM = 100$. When the value of H_g is large (Figs. 10(a) and 11(a)), the temperature difference between

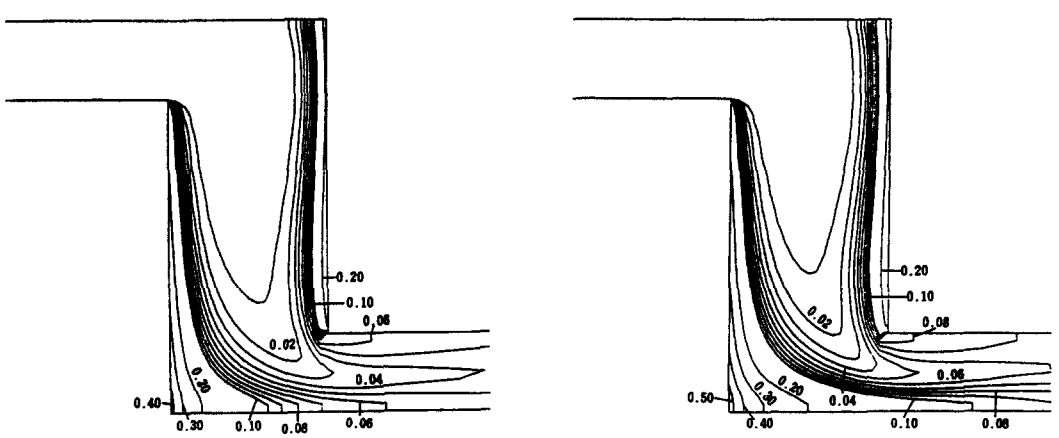

(a) RRM=1000 (b) RRM=10

Fig. 7. Dimensionless fluid temperature Θ_g ($Da = 2.5 \times 10^{-3}$, $H_g = 10$): (a) $RRM = 1000$; (b) $RRM = 10$.

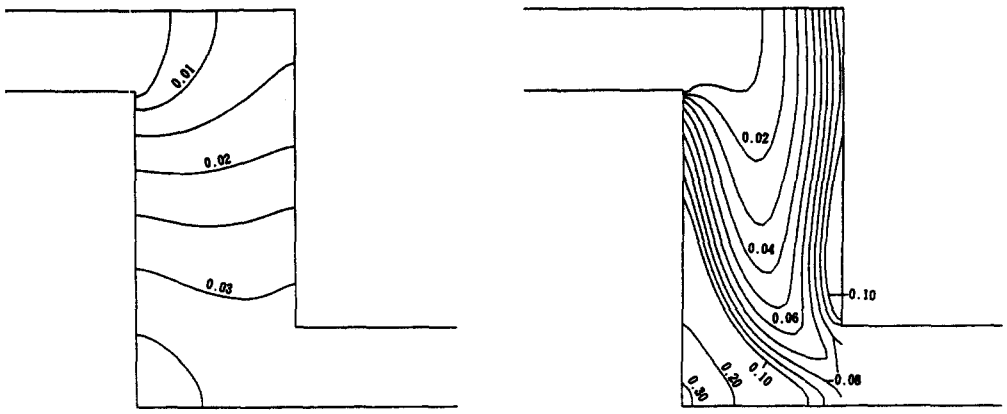

(a) RRM=1000 (b) RRM=10

Fig. 8. Dimensionless solid temperature Θ_s ($Da = 2.5 \times 10^{-3}$, $H_g = 10$): (a) $RRM = 1000$; (b) $RRM = 10$.

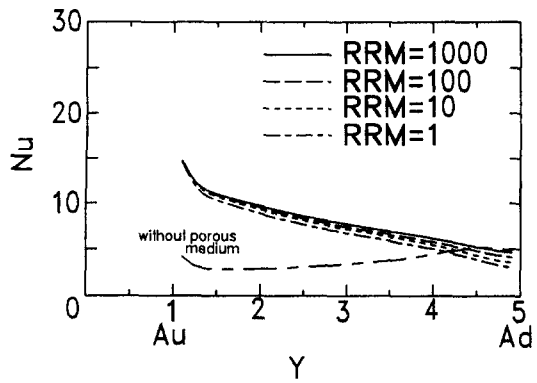

(a) (Au-Ad) side

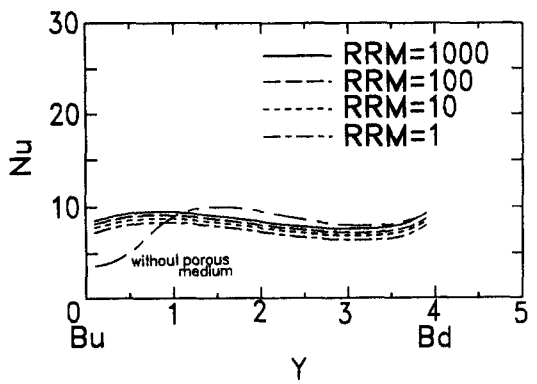

(b) (Bu-Bd) side

Fig. 9. Local Nusselt number ($Da = 2.5 \times 10^{-3}$, $H_g = 10$): (a) (Au-Ad) side; (b) (Bu-Bd) side.

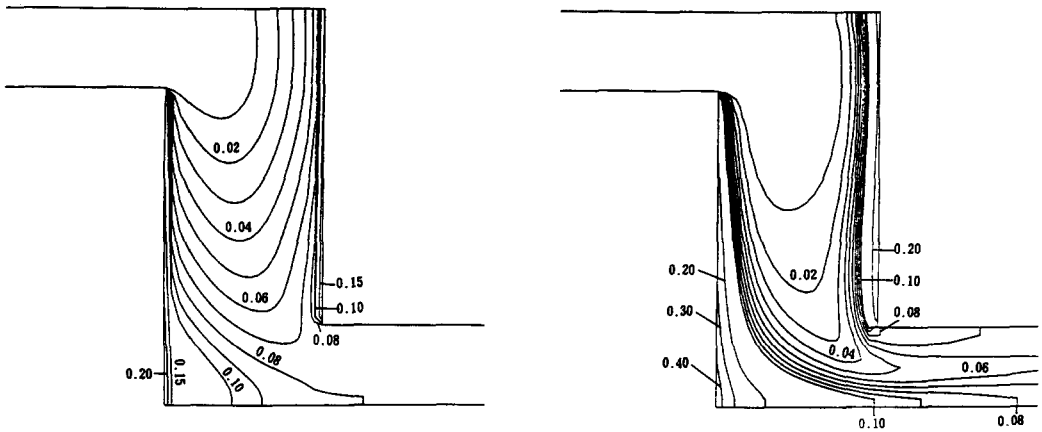

(a) Hg=1000 (b) Hg=10

Fig. 10. Dimensionless fluid temperature Θ_g ($Da = 2.5 \times 10^{-3}$, $RRM = 100$): (a) $H_g = 1000$; (b) $H_g = 10$.

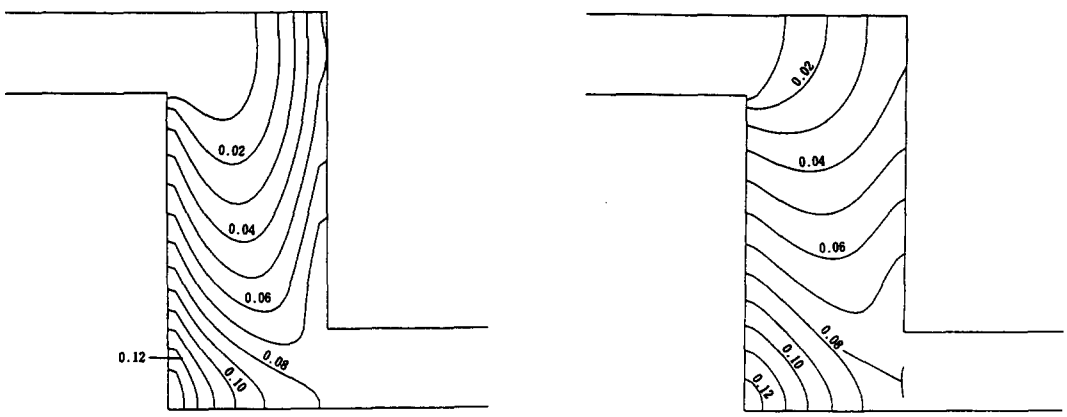

(a) Hg=1000 (b) Hg=10

Fig. 11. Dimensionless solid temperature Θ_s ($Da = 2.5 \times 10^{-3}$, $RRM = 100$): (a) $H_g = 1000$; (b) $H_g = 10$.

the porous medium and fluid is small, the temperature distribution profiles of the two phases are similar, and the thermal boundary layer is relatively thin. When the value of H_g is small, the tendency is reversed; at the center of the flow passage, the temperature of the porous medium is higher than that of the fluid. Accordingly, the local Nusselt number on the heated walls (Fig.12(a) and (b)) increases on both (Au-Ad) and (Bu-Bd) sides with the increase of H_g. When the value of H_g is varied 100-fold, the local Nusselt number increases approximately 1.7-fold on the (Bu-Bd) side. Therefore, the effect of H_g on Nu is greater than that of RRM.

Thermal performance is evaluated in Fig. 13, which shows the relationship between the mean Nusselt number ratio, Nu_m/Nu_0 and pressure drop ratio, $\Delta P/\Delta P_0$, where the subscript 0 indicates pure fluid flow in the absence of a porous medium. The solid line of inclination angle 45° means that the level of heat transfer improvement is the same as that of the pressure drop increase. The figure shows that the porous medium is effective from $Da = \infty$ to $Da = 2.5 \times 10^{-3}$ for low pressure drop and high heat transfer enhancement on the (Au-Ad) side at $Re = 300$. Thus, the effective region of high thermal performance and the value of the Da number which gives the highest value of $(Nu_m/Nu_0)/(\Delta P/\Delta P_0)$, exist for each Reynolds number. However, we should note the porous medium may suppress the heat transfer on the other (Bu-Bd) side.

CONCLUSIONS

Using a duct containing two bends, effects of a porous medium on heat transfer under forced convection were studied numerically for laminar flow.

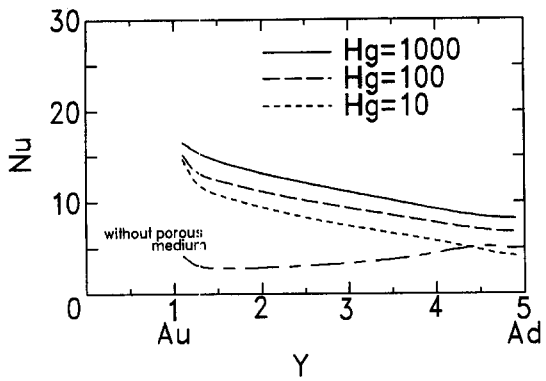

(a) (Au-Ad) side

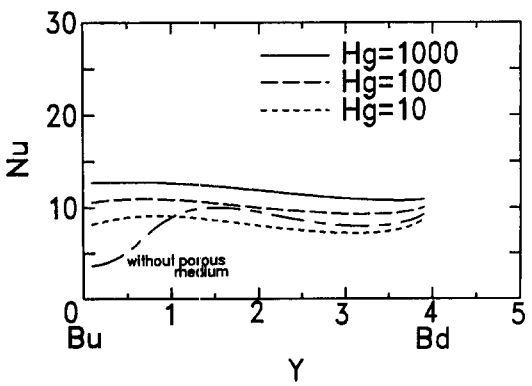

(b) (Bu-Bd) side

Fig. 12. Local Nusselt number ($Da = 2.5 \times 10^{-3}$, $RRM = 100$): (a) (Au-Ad) side; (b) (Bu-Bd) side.

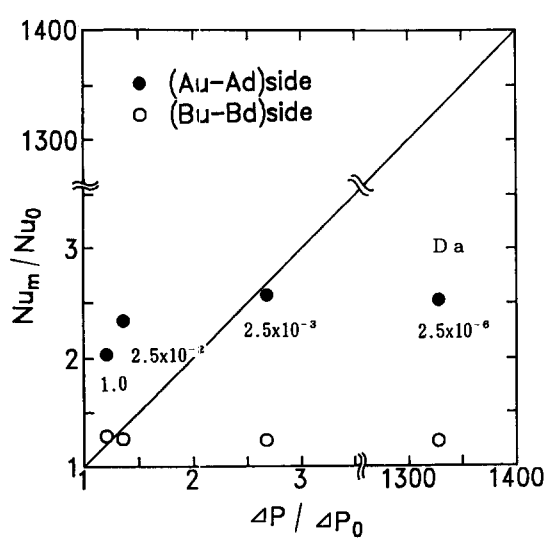

Fig. 13. Thermal performance ($Re = 300$, $H_g = 100$, $RRM = 100$).

Although the various Da numbers contributed to the development of the flow state, the flow field remains uniform throughout the vertical flow passage at $Da \leqslant 10^{-3}$; a further decrease in the Darcy number does not change the flow pattern. The ratio of thermal conductivities between the porous medium and fluid, RRM, affects the heat diffusion in the flow passage, and controls its heat storage capacity. The heat transfer parameter, H_g, between the porous medium and fluid influences the resulting temperature difference between two phases. Consequently, the local heat transfer over a section of a heated wall can be enhanced by selecting a porous medium with high values of RRM and H_g. The effective region of high heat transfer enhancement and low pressure drop and the value of Darcy number which gives the highest performance, exist for each Reynolds number. Accordingly, the results obtained in the present study can be useful for selecting a suitable porous medium for the improvement of local heat transfer in practical systems.

REFERENCES

1. Ichimiya, K. and Mitsushiro, K., Enhancement of the heat transfer of wide temperature field in a narrow flow passage (effects of porous-type turbulence promoter in normal temperature field). *Proceedings of the 1st World Conference on Experimental Heat Transfer, Fluid Mechanics and Thermodynamics*, Dubrovnik, 1988, **1**, 659–664.
2. Ichimiya, K. and Kondoh, H., Effects of a single roughness element on the heat transfer and flow situation in a parallel plate duct (numerical calculation for a porous-type and a solid-type). *Advanced Computational Methods in Heat Transfer*, 1990, **2**, 39–49.
3. Kaviany, M., Laminar flow through a porous channel bounded by isothermal parallel plates. *International Journal of Heat and Mass Transfer*, 1985, **28**(4), 851–858.
4. Kaviany, M., Boundary-layer treatment of forced convection heat transfer from a semi-infinite flat plate embedded in porous media. *Transactions of the ASME, Journal of Heat Transfer*, 1987, **109**, 345–349.
5. Poulikakos, D. and Kazmierczak, M., Forced convection in a duct partially filled with a porous material. *Transactions of the ASME, Journal of Heat Transfer*, 1987, **109**, 653–662.
6. Poulikakos, D. and Renken, K., Forced convection in a channel filled with porous medium, including the effects of flow inertia, variable porosity, and Brinkman friction. *Transactions of the ASME, Journal of Heat Transfer*, 1987, **109**, 880–888.
7. Hunt, M. L. and Tien, C. L., Effects of thermal dispersion on forced convection in fibrous media. *International Journal of Heat and Mass Transfer*, 1988, **31**(2), 301–309.
8. Vafai, K. and Tien, C. L., Boundary and inertia effects on flow and heat transfer in porous media. *International Journal of Heat and Mass Transfer*, 1981, **24**(1), 195–203.
9. Ergun, S., Fluid flow through packed columns. *Chemical Engineering Progress*, 1952, **48**(2), 89–94.
10. Golombok, M., Jariwala, H. and Shirvill, L. C., Gas-solid heat exchange in a fibrous metallic material measured by a heat regenerator technique. *International Journal of Heat and Mass Transfer*, 1990, **33**(2), 243–252.
11. Fukuda, K., Hasegawa, S. and Kondoh, T., Study on heat transfer correlation for porous media. *Transactions of JSME(B)*, 1990, **56**(529), 2729–2736.
12. Maruyama, S., Tsujino, T. and Aihara, T., Heat transfer

from a carbon fiber cluster at low Reynolds number. *Proceedings of 28th Japan National Heat Transfer Symposium*, 1991, **2**, 385–387.

13. Neal, G. and Nader, W., Practical significance of Brinkman's extension of Darcy's law: coupled parallel flows within a channel and a bounding porous medium. *The Canadian Journal of Chemical Engineering*, 1974, **52**, 475–478.
14. Gosman, A. D., Pun, W. M., Runchal, A. K., Spalding, D. B. and Wolfshtein, M., *Heat and Mass Transfer in Recirculating Flow*. Academic Press, London, 1969.